

Kinetic Modeling and Geochemical Reactions for Sequestration of CO₂ in Deep Saline Aquifer

Zerai, B., Saylor, B., Matisoff, G. and Hanson, B.

Department of Geological Sciences, 10900 Euclid Avenue, Case Western Reserve University, Cleveland, OH 44106, USA

Abstract

Kinetic modeling of the Rose Run Sandstone, a mixed silicate-carbonate deep saline aquifer, was conducted using The Geochemist's Workbench so that the timing, mass and form of CO₂ sequestration can be determined. Model conditions, among others, included rates of reactions compiled from the literature, a brine-rock ratio of 1:25, reactive rock mass based on a published Rose Run Sandstone rock composition, a brine solution of the Rose-Run Sandstone, and a CO₂ fugacity.

The kinetic modeling indicates that in the long run it should be possible to sequester large quantities of CO₂ by mineral trapping in the silicate-carbonate mineral assemblages, but in the short term it is solubility trapping that plays the most crucial role. It also indicates that the extent of mineral trapping will be sensitive to the rate of mineral-brine-CO₂ reactions relative to the rate of flow of CO₂ away from the site of injection site.

In addition, laboratory experiments were carried out to determine rates of reaction for mineral samples as functions of appropriate reaction variables. Inexpensive high-temperature and high-pressure, rocking tube reactors allow for multiple reaction experiments to run simultaneously. Dissolution rate experiments were conducted for silicate and carbonate minerals, in CO₂-pressurized KCl brine solutions, at a range of pressures and temperatures representative of deep aquifer conditions. Results from tube-reactor experiments were compared with results from experiments run under identical operating conditions in a commercial Parr stirred reactor, and with results from the published literature.

1. Introduction

There is increasing concern about the rising concentration of atmospheric carbon dioxide due to the burning of fossil fuels and its possible effect on global climate change (IPCC 2001). One option to limit the buildup of greenhouse gases in the atmosphere is to capture the CO₂ from fossil fuel-fired power plants and other point sources of greenhouse gas emissions and inject it in deep sedimentary formations, including deep, unmineable coal seams, depleted oil and gas reservoirs, and deep saline aquifers (Bachu, 2002). In the US, deep saline aquifers have a larger potential storage capacity than any other type of geological setting, with estimates as high as 500 Gt of carbon storage (Bergman and Winter, 1995). In addition to the large potential capacity, deep aquifers hold promise because they are widespread and are found in close proximity to emission sources.

The CO₂ is sequestered in deep aquifers by hydrodynamic trapping, solubility trapping, and mineral trapping (Gunter et al. 2000, Bachu and Adams 2003). Down-dip flow patterns trap CO₂ hydrodynamically by transporting it away from the surface. Solubility trapping occurs because the CO₂ reacts with the brine to form carbonic acid and other aqueous carbonate species. In dissolved form the CO₂ will not be subject to buoyancy-forces that could drive it toward the surface. In mineral trapping, the aqueous species react with mineral phases of the formation (Gunter et. al. 1997). These mineral-brine-CO₂ reactions immobilize the CO₂ by precipitating it as a solid, carbonate mineral phase (Hitchon et al 1999):



While both hydrodynamic trapping and solubility trapping may sequester significant quantities of CO₂, mineral trapping is the ultimate goal because the CO₂ is rendered harmless and immobile.

This paper presents results of kinetic modeling of a deep sandstone and carbonate aquifer beneath Ohio, USA using the computer code Geochemist's Workbench (GWB™) version 3.2.2 (Bethke, 2000) and experimental work on CO₂-brine-mineral reactions. Kinetic modeling of CO₂-brine-mineral reactions for typical mineral assemblages was applied to investigate the impact of temperature, pressure, mineralogy, brine composition, CO₂-fluid-rock ratio, and CO₂ fugacity on mineral dissolution and precipitation, amount of CO₂ sequestered, and the form of sequestration. Kinetic modeling was used to investigate chemical reactions as a function of time in order to demonstrate the impact of reaction time scale on the resulting dissolution and precipitation products. Major concerns for CO₂ sequestration in both petroleum reservoirs and aquifers requires that the geochemical models address the impacts of mineral-brine-CO₂ reactions on the integrity of the seal, the porosity of the formation near the injection site, the final minerals products, and the storage capacity of the formation. Rocking tube reactors were designed and constructed to conduct mineral-brine-CO₂ dissolution experiments at deep aquifer pressure and temperature conditions, and albite dissolution experiments were conducted for initial pressures ranging from 500 to 1300 psi and temperatures ranging from 22° to 100° C.

2. Geologic Reservoir – Rose Run Sandstone

The Cambrian Rose Run Sandstone is a deep saline aquifer and oil-gas producing unit that extends beneath eastern Ohio, Pennsylvania, New York, and Kentucky in the Appalachian Basin of Eastern United States. It is a sandy layer in the middle of the Knox Group dolomite (Janssens 1973, Riley et al., 1993) that is truncated by the Knox unconformity beneath central Ohio. The Rose Run Sandstone thickens eastward from 0 m in central Ohio to 200 m in eastern Pennsylvania. Erosional remnants and truncation along the angular unconformity form stratigraphic traps, and the subcrop belt, where the Rose Run Sandstone intersects the Knox unconformity, is the principal locale for oil and gas production.

The Rose Run Sandstone is considered a potential candidate for CO₂ sequestration because it is located beneath many of Ohio's coal-fired power plants (Fig. 1). It is also the only one of the Cambrian sandstones that is known to retain its sandstone composition in the eastern part of the state rather than passing laterally into carbonate. The Rose Run Sandstone consists of alternating layers of sandstone and carbonate. The sandstone commonly has dolomite cement and glauconite (Fig. 2). Across much of eastern Ohio the Rose Run Sandstone lies at depths suitable for injection of supercritical CO₂ (Fig. 2). The Rose Run Sandstone meets the general criteria for aquifer disposal of CO₂ outlined by Bergman and Winter (1995), Bergman et al (1997) and Bachu (2002) because it lies at depths greater than 800 m, and the regional flow is down-dip to the east and southeast (Gupta and Bair, 1997), as required for hydrodynamic trapping (Figs. 2). It is sealed by impermeable cap rock of the Trenton Limestone and Cincinnati Shales. The total thickness of these capping formations ranges from 100 to 500 m (Janssens 1973, Riley et al., 1993).

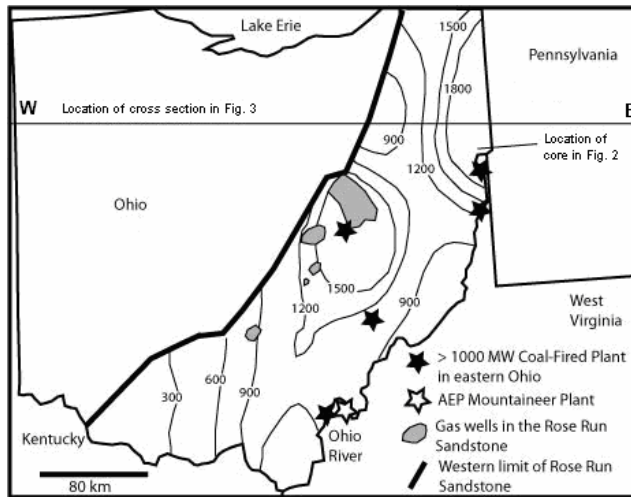


Figure 1. Map showing depth to Knox Unconformity where it overlies the Rose Run Sandstone in eastern Ohio. Contour interval in meters. AEP = American Electric Power.

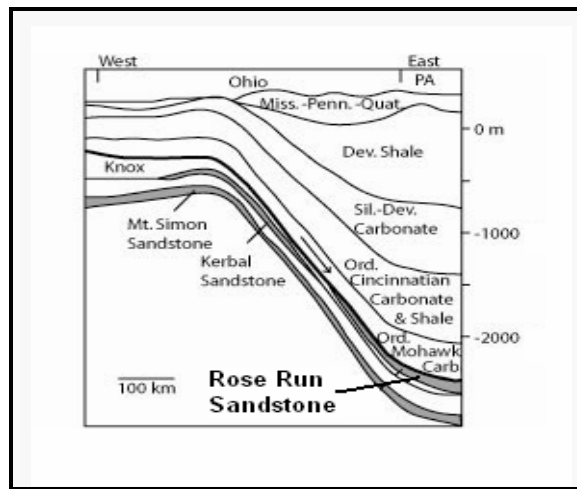


Figure 2. Cross-section for central Ohio. Cambrian sandstones that are candidates for CO₂ storage are shaded (after Gupta & Bair 1997). PA = Pennsylvania. For location of cross-section, see Figure 1.

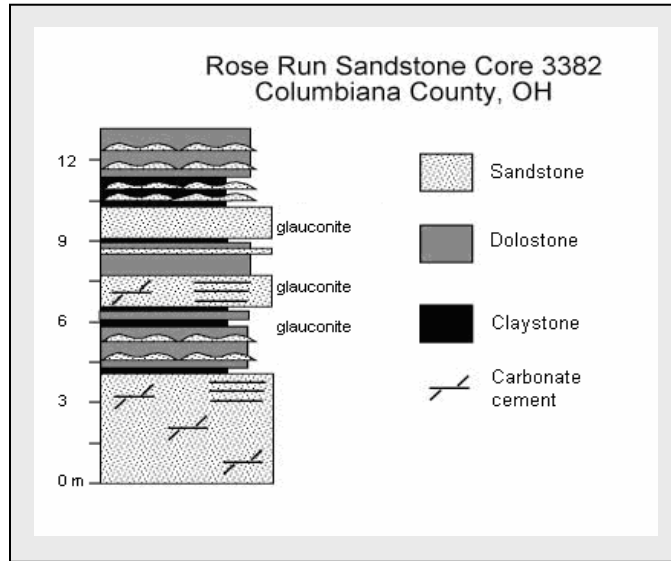


Figure 3. Measured section of core through part of the Rose Run Sandstone. For location of core, see Figure 1.

Like many deep aquifers of the eastern United States and Canada the Rose Run Sandstone consists of locally glauconitic, feldspathic quartz sandstone interbedded with dolostone and is heterogeneous at multiple scales as shown in Fig. 3 (Janssens 1973, Riley et al., 1993). The typical range of porosity and permeability of the silicate rock assemblage in the Rose Run Sandstone are 7-15% and 1-15 md, respectively (Riley et al., 1993).

3. Methods

3.1. Computer Simulation

Geochemist's Workbench (GWB™) version 3.2.2 software was used for kinetic modeling. GWB is a chemical-reactor type model that does not take into account the flow of brine. Modeling the chemical reactions under no-flow conditions provides insight into the reaction controls and the final products. It addresses geochemical effects of CO₂ injection into aquifer, and analyzes the impact of CO₂ immobilization through carbonate precipitation.

Geochemist's Workbench has an internal thermodynamic database and requires user input of kinetic rate data (Table 1). The following rate equation was adopted in the modeling (Lasaga 1995):

$$Rate = \frac{dn_i}{dt} = KA_{min} \exp\left(\frac{-E_a}{RT}\right) \left[\frac{Q}{K_{eq}} - 1\right] \quad (2)$$

where K is the rate constant (mol/cm² s), A_{min} is the reactive surface area (cm²), E_a is the activation energy (J/mol), R is the gas constant (J/k·mol), T is absolute temperature in (K), Q is the activity product, and K_{eq} is the equilibrium constant. The rate constants used here are experimentally determined and can be several

orders of magnitude greater than rates of weathering measured in the field (Lasaga, 1995). Spherical geometry of the minerals grains was assumed. The grain size of the Rose Run Sandstone is in the range of fine to medium size (Riley et al., 1993). An average grain diameter of 200 micron was assumed. Interaction with the minerals is generally expected to occur only at selective sites of the mineral surface and the difference between total surface area and reactive surface area can be between 1 to 3 orders of magnitude (Lasaga, 1995). Based on grain size the estimated reactive surface area ranges from 10 to 1000 cm²/g. A minimum calculated reactive surface area for all mineral assemblages was set at 10 cm²/g. The minimum value was chosen in order to avoid unrealistic mineral dissolution and precipitation attributed by surface area in the rate equation.

Table 1. Rate constants compiled from literature and used in the computer simulations.

Mineral	Rate constants log K (mol/m² s)	References
Albite	-11	Sverdrup, 1990
Annite	-10.5	Acker and Bricker, 1992
Calcite	-5.8	Plummer et al., 1978
Dolomite	-6.7	Busenberg and Plummer, 1982
Kaolinite	-11.4	Sverdrup, 1990
K-feldspar	-10.9	Helgeson et al., 1984
Quartz	-12	Rimstidt and Barnes, 1980

Activity coefficients were calculated using the B-dot (an extension of the Debye Huckle equation). The virial (Pitzer) method is better suited to high ionic strength solutions such as the brine under consideration, but the GWB computer code use of the Pitzer equations does not take into account the distribution of species in solution, only recognizes free ions as if each salt has fully dissociated in solution, and doesn't take into consideration SiO₂ and Al³⁺ species, precluding its use with minerals like albite, quartz, and feldspar. By using B-dot instead of Pitzer's equation, the activity coefficients for the aqueous species will be overestimated. This will have a direct impact on the amount of precipitate and dissolved minerals.

Modeled reactions with Rose Run rock aquifer consist of two types of mineral assemblages: a carbonate assemblage composed of calcite, dolomite and siderite, which represents the carbonate layers in the aquifer; and a silicate assemblage mainly composed of quartz, K-feldspar, kaolinite, albite, annite, and siderite, which represents the sandstone layers. Annite was used as a proxy in place of glauconite due to the lack of thermodynamic and kinetic data for glauconite. The abundance of each mineral phase was compiled from Janssens (1973) and Riley et al. (1993) and recast to 10 kg of rock assemblage (Table 2).

Table 2. The mineral assemblages of the Rose Run and each mineral mass recast based on a total of 10 kg rock mass.

Silicate-Carbonate	Wt %
Quartz	70
Dolomite	13.8
Calcite	8
K-feldspar	5
Annite	1
Albite	1
Kaolinite	1
Siderite	0.2

The brine solution used for the Rose Run Sandstone is based on samples from Coshocton County, Ohio (Breen et al., 1985). The brine of the Rose Run Sandstone is composed mainly of Na^+ , Cl^- , Ca^{2+} , Mg^{2+} , Br^- , K^+ , Sr^{2+} , SO_4^{2-} , Fe^{2+} , HCO_3^- , H^+ , $\text{SiO}_2(\text{aq})$, and Al^{3+} (Table 3). Sodium and chloride are the dominant chemical constituents and the median concentration of total dissolved solids is 278,000 mg/kg (Breen et al., 1985). Brine mass was set at 0.4 kg H_2O plus total dissolved solids determined by the brine chemistry. In order to attain a porosity of 10-15% of the Rose Run Sandstone, the brine to rock ratio was set at 1:25. The temperature of the system was assumed isothermal and set at 54° C. The model parameters and simulation conditions are given in Table 4.

Table 3. Composition of Rose Run brine compiled from Breen et al., 1985.

Brine (Rose Run)	
Species	(mg/kg)
Na^+	60122
K^+	3354
Ca^{2+}	37600
Mg^{2+}	5880.6
HCO_3^-	122
Cl^-	191203
SO_4^{2-}	326.4
$\text{SiO}_2(\text{aq})$	3
Al^{3+}	2.16
Fe^{2+}	140
Sr^{2+}	455.52
Br^-	3760
pH	6.4
TDS	277,571

Table 4. Values of model parameters used in the kinetic modeling.

Parameters	Description
Temperature	54°C (Isothermal)
CO ₂	Fully dissolved in the brine
Activity Coefficient (B-Dot Equation)	$\log \gamma_i = - \frac{Az_i^2 \sqrt{I}}{1 + a_i B \sqrt{I}} + \dot{B}I$
Reactive surface area	10 cm ² /g
Rate constants	Table 1
Porosity	12%
Brine – Rock ratio	1:25
Total Rock Mass	10 kg
Brine (Rose Run)	Coshocton County, Ohio
Fugacity Coefficient	$\alpha = 0.45$
CO ₂ fugacity	10 MPa

Injection pressure must be kept below lithostatic pressure to avoid pressure-induced rock fracturing, which could induce earthquakes and open pathways for the escape of CO₂. The maximum allowable injection pressure that avoids rock fracturing was specified and then based on this pressure, the maximum fugacity was calculated. In the Rose Run Sandstone, the pore pressure gradients are likely to be between 10.5 and 12.4 kPa/m (Gupta et al., 2000). The injection pressure needs to be somewhat higher than the pore pressure to force the fluids into the formations. The upper limit of the CO₂ injection pressure should not exceed 85% of the lithostatic (fracturing) pressure (Gunter et al., 2000). The lithostatic pressure in the study area ranges from 20 to 26 MPa. Using a pore pressure gradient 12 kPa/m, the injection pressure should not exceed 22 MPa for an injection depth of 1000 m.

The fugacity (f_{CO_2}) of the system at the injection site is calculated based on the following formula:

$$f_{CO_2} = \alpha P_{CO_2} \quad (3)$$

where P_{CO_2} is the injection pressure of CO₂ and is equal to the total pressure, and α is the fugacity coefficient, which depends on pressure and temperature. In this modeling the fugacity coefficient was set to 0.45, which is appropriate for $T = 54^\circ \text{C}$ and $P = 20 \text{ MPa}$ (Garrels and Christ, 1965). The initial CO₂ fugacity was set at 10 MPa in the kinetic modeling.

Simulation begins by computing the initial equilibrium state of the system. The injection of CO₂ into brine drives down the pH of the system from 6.4 to 3.9. Based on thermodynamic data of the minerals involve in the reaction, the system can be allowed to react under equilibrium condition or, using the appropriate rate constants (Table 1) and Eq. (2), it can be allowed to react kinetically. Equilibrium modeling is a critical part of understanding geologic sequestration of CO₂ because it is the best method to

predict the ultimate fate of the injected CO₂. Kinetic modeling has two advantages; it permits computing the time the system needs to start consuming CO₂ and trapping it in precipitated phase, and the time it takes the system to approach ‘steady state’ or dynamic equilibrium.

3.2. Experimental Work

Albite dissolution rate experiments were conducted in replicate for temperatures ranging between 18° and 100° C and for initial pressures ranging from 500 to 1300 psi as shown in Table 5. The experimental work was conducted using rocking tube reactors and a Parr stirred reactor. For each rocking tube experiment 1 g of the 60-90 µm size fragment of ground sieved albite was washed rinsed with nitric acid and washed in an ultrasonic acetone bath before being placed in the reactor with 150 ml of 0.7 molar KCl brine and pressurized with CO₂. The CO₂ tank was left connected to the reactor for 30 minutes in order to allow the CO₂ to come to equilibrium with the brine. The reactor was then closed and heated, and the liquid phase was sampled periodically through the duration of the experiment. In the experiment, 1 ml aliquots of brine were collected at intervals of days to weeks. The concentration of Na in the brine was measure by Atomic Absorption. The concentrations of Si and Al in the brine were measured colorimetrically. Mineral surface areas were estimated geometrically. Due to small irregularities on the surfaces of grains, geometric approximations tend to underestimate albite surface area. SEM examination of albite grains was conducted before and after experiments. To verify reproducibility, rocking tube experiments were conducted in triplicate and the results were compared to Parr experiments.

4. Results and Discussion

4.1. Kinetic Modeling

In the kinetic modeling, the initial CO₂ fugacity sets at 10 MPa, which was dissolved in the brine. Fig. 4a shows the mass of CO₂ through time. There was a rapid decline in fugacity of CO₂ as a result of reactions of the type described by Eq. (1). After 1500 years the consumption of CO₂ slows down. For example, at 100 years 20% of the CO₂ was removed from the system and precipitated as carbonate phases. Dissolve CO₂ (HCO₃⁻, H₂CO₃, CO₃²⁻) did not exceed 65 mmolal (per 10 kg of rocks) and it was trapped in precipitated carbonate minerals (Fig. 4b). In Figs. 4a and 4b positive value indicates that the dissolved carbonate species remain in the system whereas negative value indicates how much of the carbonate was removed from solution and trapped as carbonate minerals. Much of the bicarbonate formed by the dissolution of calcite was removed from the system and trapped in the precipitated dolomite phase.

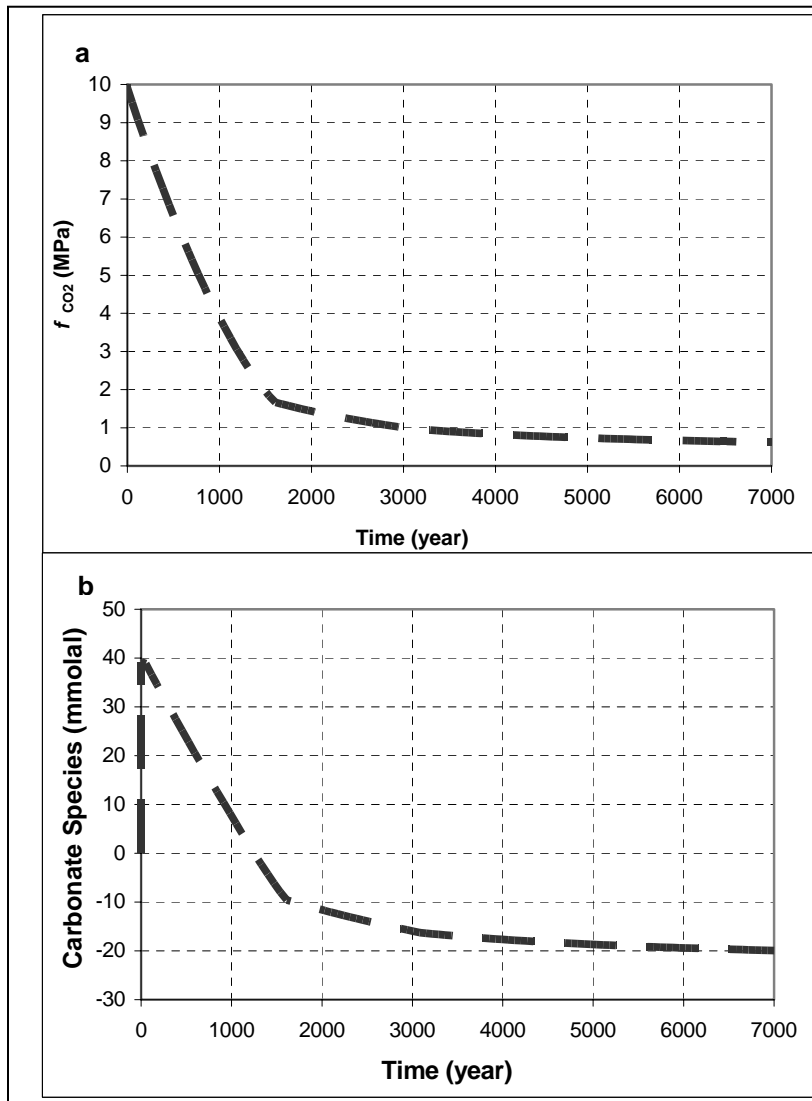


Figure 4. Fugacity of CO₂ (a), and aqueous carbonate species (b) as a function of time in kinetic model simulations.

Fig. 5 shows an overall net precipitation of siderite, dawsonite, and strontianite and the dissolution of K-feldspar, annite, albite, and kaolinite in the silicate-carbonate rock assemblages. Dawsonite has also been reported from the reaction of Na-rich brine, CO₂ and formation rocks (Johnson et al. 2001). The maximum precipitation of carbonate phases ranges from 0 to 0.6 mole of siderite, 0 to 0.4 mole of dawsonite, and 0.01 mole of strontianite. There was net rock mass gain of 30 grams (precipitation) in the silicate-carbonate assemblage, which was accompanied by a porosity drop of 0.2%. Precipitation of quartz, muscovite, and microcline were the largest contributors to the rock mass gain. The silica released from the dissolving K-feldspar, kaolinite and albite was precipitated as quartz and tridymite. The absolute abundance of quartz was much larger than the other precipitated minerals.

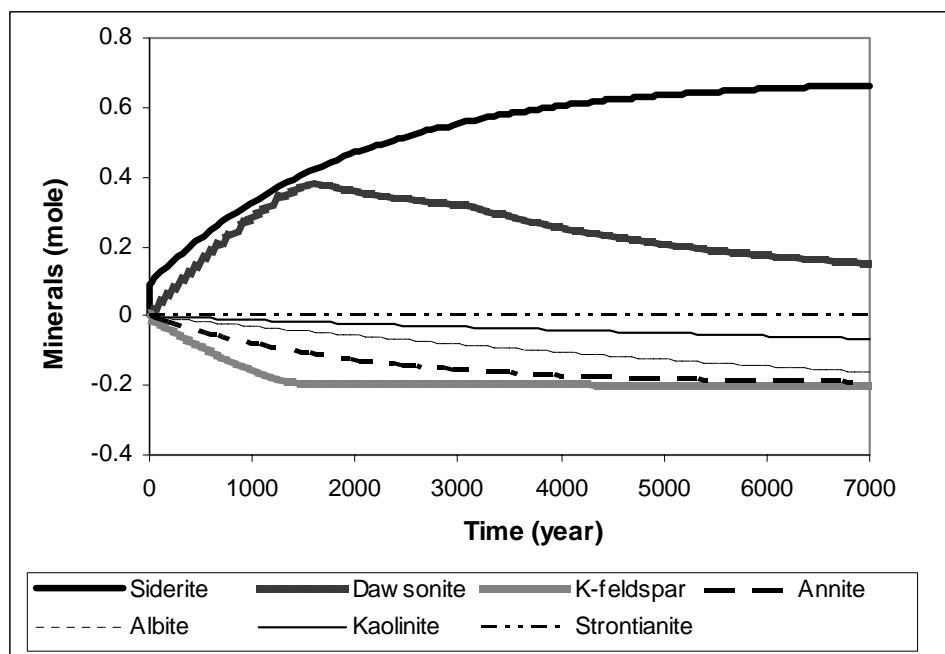


Figure 5. Computer model results of mineral precipitation/dissolution of silicate-carbonate rock assemblages.

Kinetic reaction simulations indicate that there was a small increase in pH, few years after reaction of injected CO₂, brine and rock and attain its maximum values at the end of 7000 years. Initially, the pH of the system, after injection of CO₂ was 3.9. The increase in pH through time indicates that a significant quantity of CO₂ is up taken by chemical reaction. In addition, the consumption of CO₂ was facilitated by the dissolution of albite, K-feldspar, annite and kaolinite, which eventually lead to chemical reaction between rock-CO₂-brine to produce carbonate minerals. Water-CO₂-rock reactions indicates a significant amount of CO₂ being sequestered in siderite and dawsonite (Fig. 5). The formation of both siderite and dawsonite were determined by the rate of dissolution of annite, albite and K-feldspar and the concentration of solute Na and Fe in the brine. K-feldspar was dissolved at lower pH formed by the interaction of injected CO₂ with the reservoir brine and approaches equilibrium with the solution and stops dissolving after 1000 years (Fig. 5). The Al released from the K-feldspar and kaolinite combines with Na from the brine and dissolved CO₂ to form dawsonite.

In the first few hundred years, 10-20% of the CO₂ was consumed by dissolution of silicate phases and precipitation of carbonate phases (Fig. 6). The rest remains as dissolved aqueous species. In the first thousand years, 3-4 grams of CO₂ per kg of reacted solid rock were trapped (Fig. 6). These results suggest that it is theoretically feasible to sequester large quantities of CO₂ as a carbonate mineral phases in the Rose Run Sandstone. A longer-term field and laboratory experiments is essential to test the geochemical features of CO₂ sequestration. Dissolution of CO₂, carbonate precipitation, and a drop in pH were confirmed experimentally at 200° C and 20 MPa by Kaszuba et al. (2003). The mineral trapping of CO₂ is a long-term, on-going process that will evolve as solution chemistry evolves over time and minerals

evolve in response to the fluid chemistry changes. Calculation predictions need to be tested in experiments to determine if carbonate minerals would form under specific laboratory conditions as predicted by the modeling.

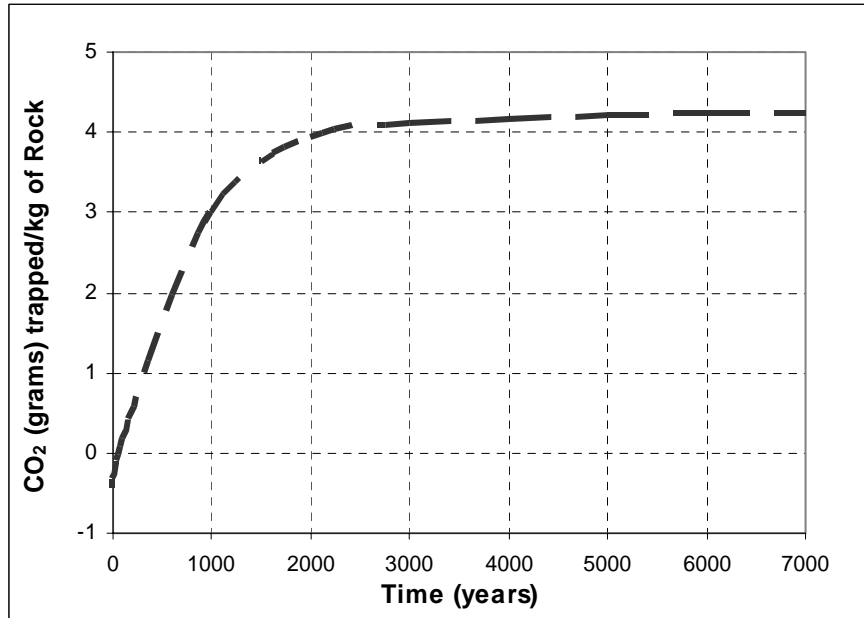


Figure 6. Total CO₂ uptake during the brine-rock-gas reaction for brine-rock ratio of 1:25 and $\phi = 12\%$.

4.2. Experimental Results on Albite Dissolution

The experimental work on whole Rose Run Sandstone is on-going process and in this paper we only report the dissolution of albite for single mineral experiment. Fig. 7 shows the concentration of Na over time for the initial stages of low (18-22°C) temperature experiments H1 and H2 and medium (75°C) temperature experiments F1 and G1. During their initial phases these experiments are expected to follow a linear rate law:

$$C = C_0 + kt \quad (4)$$

where k is the rate constant in units of moles/L/time and t is time. The far-from-equilibrium mineral dissolution rate is obtained by dividing by the volume of brine and the mineral surface area. Mineral dissolution rates calculated from Na concentration data are shown in Table 5. These rates agree with published albite dissolution rates for neutral pH. They differ by nearly 2 orders of magnitude between replicate experiments conducted at 22° C and replicate experiments conducted at 75° C reflecting the effect of temperature on dissolution rate. Based on the temperature dependence of dissolution rate the activation energy can be calculated using:

$$E_a = -2.3026 \times R (\log K_1 - \log K_2) / (1/T_1 - 1/T_2) \quad (5)$$

For comparison of experiments F1 and H1 and for comparison of experiments F1 and H2 calculated $E_a = 37$ and 48 KJ/mol respectively.

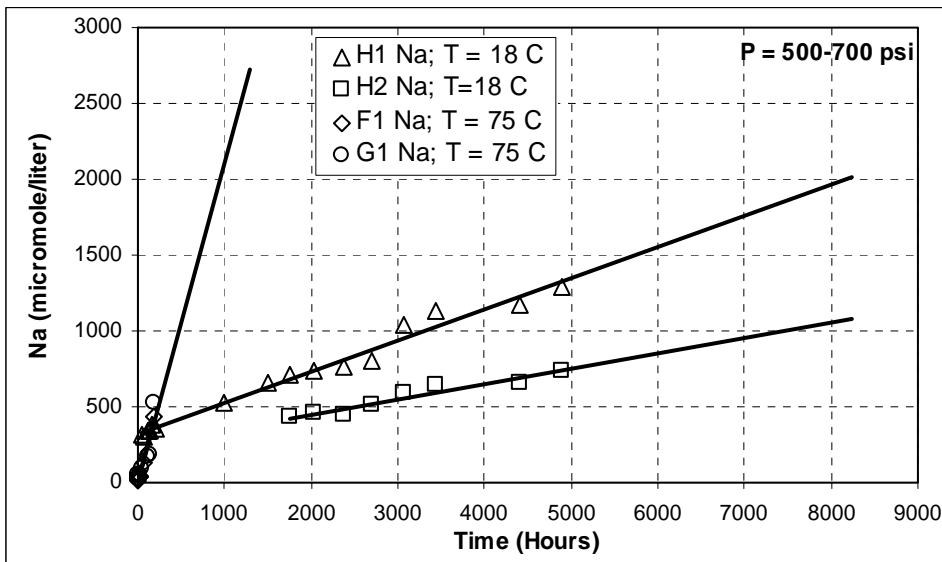


Figure 7. Sodium (Na) concentration for initial, far-from-equilibrium stage of albite dissolution experiments.

Table 5. Albite dissolutions rates as determined from Na (Fig. 7) and Si (Fig. 8).

Experiment	Log Na rate (mol/m ² /sec)	Log Si rate (mol/m ² /sec)
F1	-10.7	
G1	-10.7	
H1	-11.7	-12.2
H2	-12	-12.5
M1		-12
M2		-12.2
I1	-11.1	
I2	-11	

Fig. 8 shows Si concentration over time for low (500-700 psi) initial pressure experiments H1 and H2 and for medium (700-900 psi) and high (900-1300 psi) initial pressure experiments M1 and M2. Only the low temperature experiments yield linear Si concentration data during the initial stages. The higher temperature experiments quickly saturate with respect to Si and curve. Dissolution rates calculated based on Si concentration data (Table 5) compare well with rates calculated for Na concentration data for experiments H1 and H2. In addition, dissolution rates calculated for H1 and H2 agree well with rates calculated for M1 and M2, even though initial pressures of CO₂ varied by more than 400 psi. The small variation in rate may reflect the effect of pH values close to 6. In that range, the dissolution rates of feldspar are largely independent of pH.

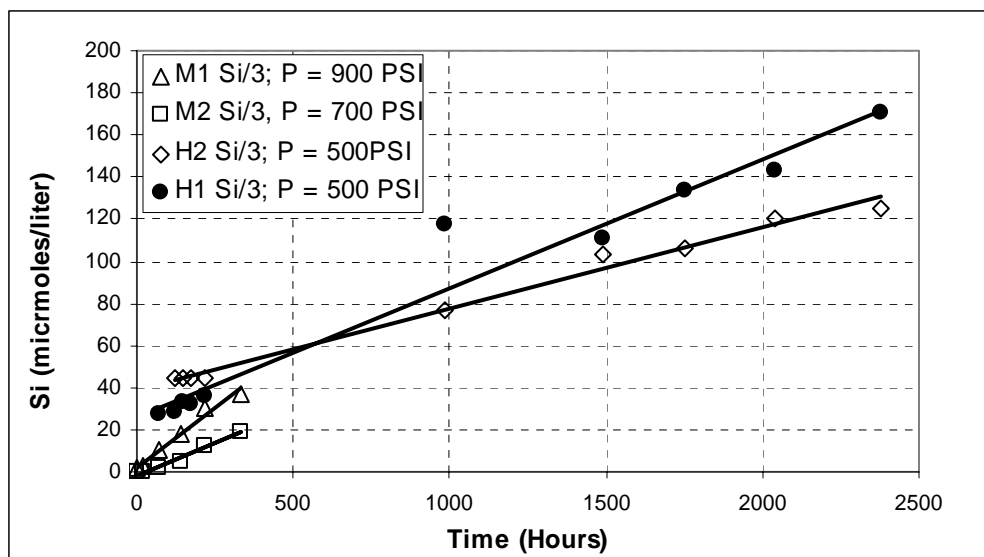


Figure 8. Silica (Si) concentration for far-from-saturation stage of albite dissolution experiments.

Estimation of Storage Capacity

Table 6 compares the density in pure form and the effective storage density (kg of CO₂/m³ rock) for the different mechanisms of trapping CO₂ estimated for the Rose Run Sandstone. Although the density of CO₂ in free, aqueous, and mineral forms differs by two orders of magnitude, there is substantial overlap of estimated effective storage density for the formation. Stated another way, according to these estimates, all the free CO₂ that can be injected into a formation, if converted to aqueous or mineral form would cover close to the same volume of the aquifer as that covered by the injection plume. For the 60 m thick Rose Run Sandstone the volume necessary to store 30 years of emissions from a 1000 MW power plant (330 Mtons) has a radius of 11-26 kilometers. Since the five largest coal-fired power plants in Eastern Ohio are spaced on the order of 50 miles apart the Rose Run Sandstone has the potential to receive 30 years of their CO₂ emissions and to store them over millennia as a negatively buoyant aqueous solution and, ultimately, as immobile carbonate mineral.

Table 6. Capacity of different mechanisms to store CO₂.

CO ₂ trapping mechanism	CO ₂ density at 10 MPa, 35°C	Average storage density in aquifer at 10 MPa, 35°C, 10% porosity and	Radius and height of storage volume for 330 Mtons CO ₂
Hydrodynamic	700 kg/m ³	20% saturation: 14 kg/m ³ 6% saturation: 5 kg/m ³	H = 60 m R = 11 km – 18 km
Solubility	40 kg/m ³	4 kg/m ³	H = 60 m R = 21 km
Mineral	CO ₂ in calcite 1250 kg/m ³	10 MPa fCO ₂ : 26 kg/m ³ 2 MPa fCO ₂ : 5 kg/m ³	H = 30 m (sandstone layers only) R = 11 – 26 km

5. Conclusion

Computer simulations using the computer program 'Geochemist's Workbench' used to model the kinetic assemblages produced by reacting typical Rose Run silicate and carbonate mineral assemblages with measured brine compositions. This modeling of the chemical reactions under no-flow conditions provides insight into what parameters control the reactions and their final products. The results demonstrate that dissolution of albite, K-feldspar, and glauconite and the precipitation of siderite and dawsonite are potentially very important for mineral trapping of CO₂. The kinetic modeling indicates that over hundreds to thousands of years it should be possible to sequester large quantities of CO₂ by mineral trapping in the silicate-carbonate units of the Rose Run Sandstone, but over tens to hundreds of years solubility trapping plays the most crucial role. This work demonstrates that the Rose Run Sandstone has a suitable mineral composition for significant mineral trapping of CO₂. However, the extent of mineral trapping will be sensitive to the rate of mineral-brine-CO₂ reactions relative to the rate of flow of CO₂ away from the site of injection. Reactions must be fast enough to reach carbonate phase saturation before the CO₂ is overly diluted by outward radial flow and diffusion. On the other hand, quartz and other silicate minerals are by far the dominant phases precipitated as a result of the reactions and, if the reactions are fast enough, quartz has the potential to clog the well during CO₂ injection.

Dissolution rate of albite in high pressure and temperature was carried out. Mineral dissolution rates calculated from Na concentration data agree with published albite dissolution rates for neutral pH. The nearly two orders of magnitude difference between replicate experiments conducted at 22° C and replicate experiments conducted at 75° C reflects the effect of temperature on dissolution rate. Dissolution rates calculated based on Si concentration compare well with rates calculated based on Na concentration for experiments H1 and H2. In addition, dissolution rates were calculated and their results were compared between experiments that had different initial pressures and good agreement was found.

References

- Acker, J.G., and Bricker, O.P., 1992. The Influence of pH on Biotite Dissolution and Alteration Kinetics at Low Temperature. *Geochim. Cosmochim. Acta* 56:3073-3092.
- Bachu, S., 2002. Sequestration of CO₂ in Geological Media in Response to Climate Change: Road Map for Site Selection using the Transform of the Geological Space into CO₂ Phase Space, 43: 87-102.
- Bachu, S., and Adams, J.J. 2003. Sequestration of CO₂ in Geological Media in Response to Climate Change: Capacity of Deep Saline Aquifers to Sequester CO₂ in Solution. *Energy Convers. Mgmt.* 44: 3151-3175.
- Bergman, P. D., Winter, E. M., and Chen, Z. Y. 1997. Disposal of Power Plant CO₂ in Depleted Oil and Gas Reservoirs in Texas. *Energy Convers. Mgmt.* 38: S211-S216
- Bergman, P. D., and Winter, E. M. 1995. Disposal of CO₂ in Aquifers in the U.S. *Energy Convers. Mgmt.* 36: 523-526.
- Bethke, C. M. 2000. The Geochemical WorkBench (GWB) Version 3.2.2. A Users Guide to Rxn, Act2, Tact, React, and Gtplot. Craig Bethke and the Board of Trustees of the University of Illinois.
- Breen, Kevin J et al., 1985. USGS Water Resources Investigation Report (84-4314), Ohio Department of Natural Resources Division of Oil and Gas.
- Busenberg, E., and Plummer, L.N., 1982. The Kinetics of Dissolution of Dolomite in CO₂-H₂O Systems at 1.5-65° C and 0-1.0 atm P_{CO₂}. *Am. J. Sci.* 282:45-78.
- Garrels, R.M., and Christ, C.L. 1965. *Solutions, Minerals, and Equilibria*. Harper & Row Publisher, New York. P 20-73.
- Gunter, W. D., Wiwchar, B., and Perkins, E. H. 1997. Aquifer Disposal of CO₂-rich Greenhouse Gases: Extension of the Time Scale of Experiment for CO₂-Sequestering Reactions by Geochemical Modeling. *Mineralogy and Petrology*. 59: 121-140.
- Gunter, W. D., Perkins, E. H., and Hutcheon, I. 2000. Aquifer Disposal of Acid Gases: Modeling of Water-Rock Reactions for Trapping of Acid Wastes. *Applied Geochemistry*. 15: 1085-1095.
- Gupta, N., and Bair, E. S. 1997. Variable-Density Flow in the Midcontinental Basin and Arches Region of the United States. *Water Resources Research*. 33: 1785-1802.
- Gupta, N., and S., Sminchak, J., 2000. Simulation of CO₂ Sequestration in Deep Saline Formations in the Midwest. Battelle Report Prepared for US DOE, National Energy Tech. Lab., Contact: DE-AF26-99FT00486. December 22.
- Helgeson, H.C., Murphy, W.M., and Aagaard, P., 1984. Thermodynamics and Kinetic Constraints on Reaction Rates Among Mineral and Aqueous Solutions. II. Rate Constants, Effective Surface Area, and the Hydrolysis of Feldspar. *Geochim. Cosmochim. Acta* 48:2405-2432.
- Hitchon, B., Gunter, W.D., Gentzis, T., and Bailey, R.T. 1999. Sedimentary Basins and Greenhouse Gases: A Serendipitous Association. *Energy Convers. Mgmt.*, 40: 825-843.
- IPCC. 2001. *Climate Change 2001: Synthesis Report*.

- Janssens, A., 1973, Stratigraphy of the Cambrian and Lower Ordovician Rocks of Ohio, Ohio Department of Natural Resources, Division of the Geological Survey, Bulletin 64, 197 p.
- Johnson, J. W., Nitao, J. J., Steefel, C. I., and Knauss, K. G. 2001. Reactive Transport Modeling of Geologic CO₂ Sequestration in Saline Aquifers: The Influence of Intra-Aquifer Shales and the Relative Effectiveness of Structural, Solubility, and Mineral Trapping during Prograde and Retrograde Sequestration. AGU Meeting Washington DC.
- Kaszuba, P.J., Janecky, R.D., and Snow, G.M., 2003. Carbon Dioxide Reaction Processes in a Model Brine Aquifer at 200° C and 200 bars: Implications for Geologic Sequestration of Carbon. *Applied Geochemistry* 18:1065-1080.
- Lasaga, A.C. 1995. Fundamental Approaches in Describing Mineral Dissolution and Precipitation Rates. In 'Chemical Weathering Rates of Silicates Minerals'. Ed. A.F. White and S.L. Brantley. *Reviews in Mineralogy*. V. 31:23-86
- Plummer, L.N., Parkhurst, D.L., and Wigley, T.M.L., 1978. The Kinetics of Calcite Dissolution in CO₂-Water Systems at 5-60° C and 0.0-1.0 atm CO₂. *Amer. J. Sci.* 278:176-216.
- Riley, R. A., Harper, J. A., Baranoski, M. T., Laughrey, C. D., and Carlton, R. W. 1993. Measuring and Predicting Reservoir Heterogeneity in Complex Deposystems: The Late Cambrian Rose Run Sandstone of Eastern Ohio and Western Pennsylvania. US Department of Energy, pp. 257.
- Rimstidt, J.D., and Barnes, H.L., 1980. The Kinetics of Silica-Water Reactions. *Geochim. Cosmochim. Acta* 44:1683-1699.
- Sverdrup, H.U., 1990. The Kinetics of Base Cation Release due to Chemical Weathering. Lund University Press, Lund